Kinetic Studies of Thymidine Phosphorylase from Mouse Liver[†]

Max H. Iltzsch,[‡] Mahmoud H. el Kouni, and Sungman Cha*

Division of Biology and Medicine, Brown University, Providence, Rhode Island 02912

Received January 8, 1985

ABSTRACT: Initial velocity and product inhibition studies of thymidine phosphorylase from mouse liver revealed that the basic reaction mechanism of this enzyme is a rapid equilibrium random bi-bi mechanism with an enzyme–phosphate–thymine dead-end complex. Thymine displayed both substrate inhibition and nonlinear product inhibition, i.e., slope and intercept replots vs. 1/[thymine] were nonlinear, indicating that there is more than one binding site on the enzyme for thymine and that when thymine is bound to one of these sites, the enzyme is inhibited. Furthermore, both thymidine and phosphate showed "cooperative effects" in the presence of thymine at concentrations above 60 μM, suggesting that the enzyme may have multiple interacting allosteric and/or catalytic sites. The deoxyribosyl transferase reaction catalyzed by this enzyme is phosphate-dependent, requires nonstoichiometric amounts of phosphate, and can proceed by an "enzyme-bound" 2-deoxyribose 1-phosphate intermediate. These findings are in accord with the rapid equilibrium random bi-bi mechanism and demonstrate that deoxyribosyl transfer by this enzyme involves an indirect-transfer mechanism. These results strongly suggest that phosphorolysis and deoxyribosyl transfer are catalyzed by the same site on thymidine phosphorylase.

Thymidine phosphorylase (thymidine:orthophosphate deoxyribosyltransferase, EC 2.4.2.4) catalyzes the reversible phosphorolysis of thymidine (dThd),[1] deoxyuridine, and their analogues (but not deoxycytidine) to their respective bases and 2-deoxyribose 1-phosphate (dRib-1-P):

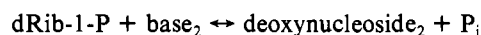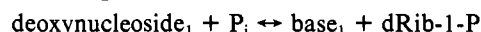$$\text{deoxynucleoside} + P_i \leftrightarrow \text{base} + \text{dRib-1-P}$$
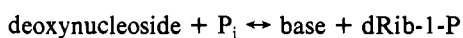
This reaction was thought to be specific for pyrimidine 2'-deoxyribonucleosides, as pyrimidine ribonucleosides are not cleaved by this enzyme (Krenitsky et al., 1964; Zimmerman & Seidenberg, 1964; Nakayama et al., 1980; Niedzwicki et al., 1983). However, Kono et al. (1983) and Iltzsch et al. (1985) have shown that the enzyme from a human lung tumor and mouse liver also cleaves 5'-deoxy-5-fluorouridine.

Thymidine phosphorylase also catalyzes a deoxyribosyl-transfer reaction that involves the transfer of the deoxyribose moiety of one deoxynucleoside, to a base, to form a second deoxynucleoside (Zimmerman, 1964; Zimmerman & Seidenberg, 1964; Gallo et al., 1967; Gallo & Breitman, 1968; Krenitsky, 1968). There are two mechanisms by which deoxyribosyl transfer can take place, direct and indirect (Krenitsky, 1968). Direct transfer involves the transfer of the deoxyribose moiety from deoxynucleoside₁, directly to base₂, to form deoxynucleoside₂:

$$\text{deoxynucleoside}_1 + \text{base}_2 \leftrightarrow \text{deoxynucleoside}_2 + \text{base}_1$$
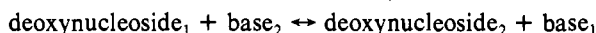
Gallo et al. (1967) and Gallo & Breitman (1968) proposed that deoxyribosyl transfer by thymidine phosphorylase from human leukocytes proceeds via the direct mechanism. Indirect transfer, on the other hand, involves the initial phosphorolysis of deoxynucleoside₁ to form base₁ and either free or enzyme-bound dRib-1-P, which then reacts with base₂ to form deoxynucleoside₂:

$$\text{deoxynucleoside}_1 + P_i \leftrightarrow \text{base}_1 + \text{dRib-1-P}$$

$$\text{dRib-1-P} + \text{base}_2 \leftrightarrow \text{deoxynucleoside}_2 + P_i$$

The net result of this reaction is the same as the direct-transfer reaction, except that the indirect-transfer mechanism is phosphate-dependent, whereas direct transfer is not. Thymidine phosphorylases from *Escherichia coli* (Schwartz, 1971) and rabbit small intestine (Krenitsky, 1968) have been shown to catalyze deoxyribosyl transfer by the indirect mechanism.

The reaction mechanism of thymidine phosphorylase has been elucidated for the enzyme from two bacterial sources, *E. coli* (Schwartz, 1971) and *Salmonella typhimurium* (Blank & Hoffee, 1975). In both cases, an ordered sequential bi-bi mechanism was postulated. In the case of the *E. coli* enzyme, however, phosphate and dRib-1-P were found to bind to free enzyme, whereas, in the case of the *S. typhimurium* enzyme, dThd and thymine (Thy) bind to free enzyme. In contrast to the bacterial enzymes, kinetic studies of mammalian thymidine phosphorylase have been rudimentary, despite the fact that this enzyme has been partially purified from a variety of mammalian sources (Friedkin & Roberts, 1954; Zimmerman, 1962; Krenitsky et al., 1964; Zimmerman, 1964; Gallo & Breitman, 1968; Krenitsky, 1968; Lyon, 1968; Gallo & Perry, 1969), purified to near homogeneity (>95% pure) from human amniochorion (Kubilus et al., 1978) and human platelets (Desgranges et al., 1981), and apparent homogeneity from horse erythrocytes (Ferone et al., 1975).

In the present investigation, detailed kinetic studies of a mammalian thymidine phosphorylase (mouse liver) were conducted in an effort to elucidate the reaction mechanism of this enzyme. In addition, the deoxyribosyl-transfer reaction catalyzed by this enzyme was examined to determine whether or not it proceeds by the direct- or indirect-transfer mechanism. A preliminary report has been presented (Iltzsch et al., 1985).

[‡] Present address: Department of Pharmacology, Stanford University School of Medicine, Stanford, CA 94305.

[1] Abbreviations: dRib-1-P, α-D-2-deoxyribose 1-phosphate; dThd, thymidine; P_i, orthophosphate; Thy, thymine.

EXPERIMENTAL PROCEDURES

Materials. [2-^{14}C]Thd (56 Ci/mol) was obtained from Moravek Biochemicals Inc., Brea, CA; [2-^{14}C]Thy (55.2 Ci/mol) and Omnifluor scintillant were from New England Nuclear Corp., Boston, MA; [U-^{14}C]dThd (528 Ci/mol) was from Amersham Corp., Arlington Heights, IL; protein assay kits were from Bio-Rad Laboratories, Richmond, CA; silica gel G/UV$_{254}$ polygram thin-layer chromatography plates were from Brinkmann, Westbury, NJ. All other materials were obtained from Sigma Chemical Co., St. Louis, MO.

Purification of Thymidine Phosphorylase. Thymidine phosphorylase was partially purified from mouse liver (CD-1 mice) by DEAE-cellulose, phenyl-Sepharose CL-4B, Dye-matrex Red A, and hydroxylapatite column chromatographic techniques. This procedure resulted in a 175-fold purification of the enzyme over the homogenate with a specific activity of 0.11 μmol/min^{-1} (mg of protein)$^{-1}$ and a yield of 39%. This enzyme preparation is free of all possible enzymes that might interfere with the assay of thymidine phosphorylase activity, namely, dihydrouracil dehydrogenase (EC 1.3.1.2), purine-nucleoside phosphorylase (EC 2.4.2.1), uridine phosphorylase (EC 2.4.2.3), thymidine kinase (EC 2.7.2.1), phosphodeoxy-ribomutase (EC 2.7.5.6), and nonspecific phosphatase (EC 3.1.3.-). Details are described elsewhere (Iltzsch, 1985).

Enzyme Assays. dThd cleavage was measured by following the formation of [2-^{14}C]Thy from [2-^{14}C]dThd in the presence of phosphate (pH 7.4); dThd synthesis was measured by following the formation of [2-^{14}C]dThd from [2-^{14}C]Thy and dRib-1-P, and deoxyribosyl transferase activity was determined by measuring the formation of [2-^{14}C]dThd from [2-^{14}C]Thy in the presence of unlabeled dThd. All assays contained 50 mM imidazole hydrochloride, pH 7.4, 0.5 mM dithiothreitol, varied amounts of substrates, and either 1.5×10^{-4} (nucleoside synthesis) or 6.4×10^{-4} unit (all other assays) of enzyme, in a final volume of 140 μL. Reactions were started by the addition of enzyme, incubated at 37 °C for 10 min, during which the reaction was linear, and terminated by placing the reaction tube in a boiling water bath for 1 min. Proteins were removed by centrifugation; then 10 μL of the resulting supernatant fluid was added to 10 μL of a standard solution containing 10 mM each of Thy and dThd. This mixture was spotted on silica gel plates, which were then developed with chloroform–methanol–acetic acid (90:10:1 v/v/v). R_f values were 0.38 and 0.7 for dThd and Thy, respectively. In the study in which [U-^{14}C]dThd was used as a substrate, the plates were developed in chloroform–methanol (9:1 v/v), and R_f values were 0, 0.4, and 0.7 for dRib-1-P, dThd, and Thy, respectively. Initially, dRib-1-P was identified by spraying the plates with the diphenylamine reagent described below; however, in subsequent experiments, the origin was simply cut out without spraying the plates. dThd and Thy were identified by UV quenching. Spots were cut out and counted in 20 mL of Omnifluor scintillation fluid in a Packard Tri-Carb 460C liquid scintillation counter.

When product inhibition studies were conducted with Thy as the product inhibitor, a spectrophotometric assay was employed, which measures dRib-1-P formation from dThd. This assay was used in lieu of the radioisotopic assay, because addition of unlabeled Thy increased the formation of radiolabeled dThd by the deoxyribosyl transferase reaction. The assay mixture contained 50 mM imidazole hydrochloride, pH 7.4, 0.5 mM dithiothreitol, varied amounts of potassium phosphate (pH 7.4), dThd and Thy, and 9.1×10^{-4} unit of enzyme, in a final volume of 400 μL. A modification of the method of Giles & Myers (1965) was employed to measure
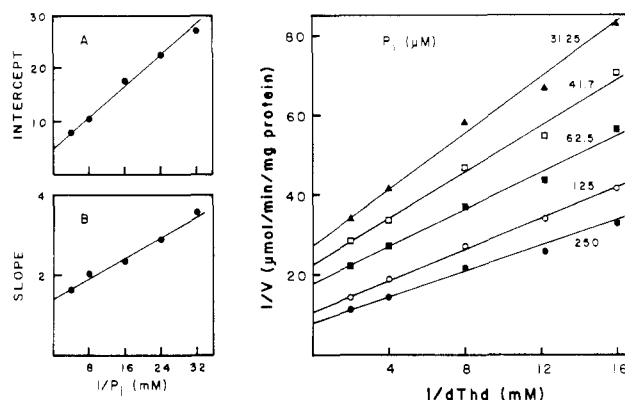

FIGURE 1: Initial velocity studies. Plots of 1/velocity vs. 1/[dThd] at various fixed concentrations of phosphate. The common intersecting point was estimated at coordinates -11.5 ± 0.9 and -1.12 ± 0.003. $K_{\mathrm{dThd}} = 288.6 \pm 23.5 \mu$M and $K_{\mathrm{i,dThd}} = 87.2 \pm 11.3 \mu$M were estimated from the replots.
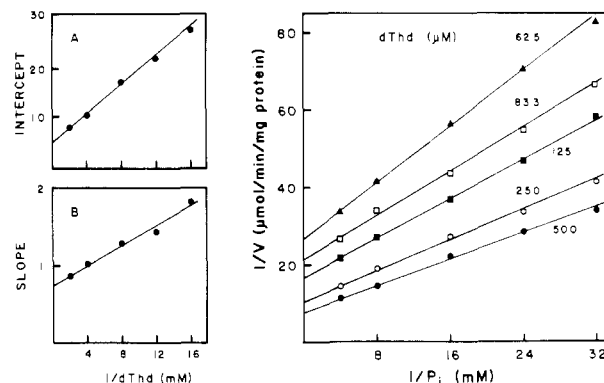

FIGURE 2: Initial velocity studies. Plots of 1/velocity vs. 1/[P$_i$] at various fixed concentrations of dThd. The common intersecting point was estimated at coordinates -21.9 ± 1.8 and -1.12 ± 0.003. $K_{\mathrm{P_i}} = 151.2 \pm 12.2 \mu$M and $K_{\mathrm{i,P_i}} = 15.7 \pm 6.1 \mu$M were estimated from the replots.

dRib-1-P formation; 100 μL of 50% perchloric acid, 500 μL of 4% diphenylamine in acetic acid, and 25 μL of 1.6% aqueous acetaldehyde were added to the reaction tubes. The tubes were then vortexed and incubated overnight ($\sim$15–17 h) at 30 °C. The color density was measured at 595 nm in a Gilford 240 spectrophotometer. A standard curve from 5–40 nmol of dRib-1-P was used to quantitate the absorbance readings.

Calculations and Protein Determination. All statistical analyses of the kinetic data were performed with a computer program that employs the general methods of Wilkinson (1961) and Cleland (1967). Protein concentrations were determined by the method of Bradford (1976), as described by Bio-Rad Laboratories (1979), using bovine γ-globulin as a standard.

RESULTS

Kinetic Studies

The derivation of a rate equation for thymidine phosphorylase, according to the scheme shown in Figure 13, is presented in the Appendix. In the following analysis, eq 1–8 refer to equations in the Appendix. The meanings of the symbols A, B, P, and Q are given in the legend to Figure 13.

Initial Velocity Studies. Figures 1–4 show the results of the initial velocity studies. In all cases, an intersecting pattern of lines was observed in which both the intercepts and slopes changed and the common intersection point of the lines occurred below the x axis (except Figure 3, see below). These results indicate that the mechanism of thymidine phosphorylase
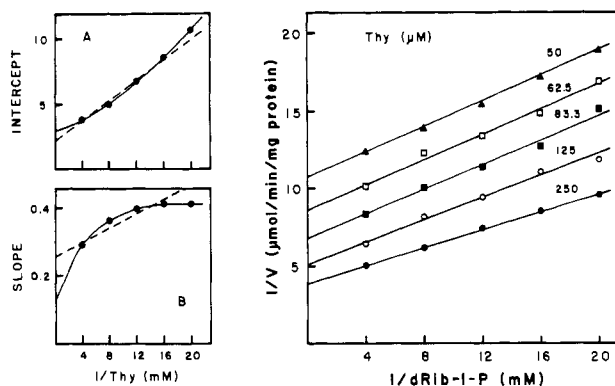
FIGURE 3: Initial velocity studies. Plots of 1/velocity vs. 1/[dRib-1-P] at various fixed concentrations of Thy. The common intersecting point was estimated at coordinates -36.9 ± 3.4 and -0.0072 ± 0.0024. Note that the standard errors, especially that of the y coordinate, are relatively high, reflecting the horizontal portion of the slope vs. 1/[Thy] replot. $K_{Thy} = 174.6 \pm 16.1$ μM and $K_{i,Thy} = 41.5 \pm 8.8$ μM were estimated from the replots.
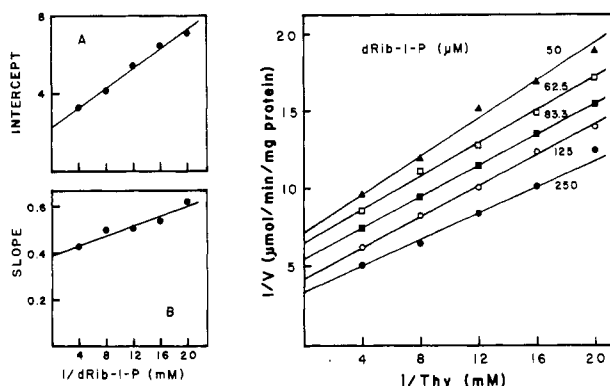

FIGURE 4: Initial velocity studies. Plots of 1/velocity vs. 1/[Thy] at various fixed concentrations of dRib-1-P. The common intersecting point was estimated at coordinates -24.1 ± 2.5 and -7.15 ± 0.002. $K_{dR-1-P} = 114.0 \pm 11.9$ μM and $K_{i,dR-1-P} = 27.1 \pm 5.5$ μM were estimated from the replots.

is sequential rather than ping-pong. These data were analyzed in detail according to the rate equation (eq 3) derived in the Appendix.

(A) dThd and Phosphate as Substrates. When dThd (A) and phosphate (B) are substrates at [dRib-1-P] = [Thy] = 0, a double-reciprocal form of eq 3 can be represented by either

$$1/v = \frac{K_a}{V_1}\left(1 + \frac{K_{ib}}{[B]}\right)\frac{1}{[A]} + \frac{1}{V_1}\left(1 + \frac{K_b}{[B]}\right) \qquad (9)$$

or

$$1/v = \frac{K_b}{V_1}\left(1 + \frac{K_{ia}}{[A]}\right)\frac{1}{[B]} + \frac{1}{V_1}\left(1 + \frac{K_a}{[A]}\right) \qquad (10)$$

from the identity relationship $K_a K_{ib} = K_b K_{ia}$. Equations 9 and 10 indicate that the initial velocity plots, as well as slope and intercept replots (vs. 1/[dThd] or 1/[P$_i$]), should be linear when dThd and phosphate are the substrates. This was indeed the case as can be seen in Figures 1 and 2.

(B) Thy and dRib-1-P as Substrates. (1) dRib-1-P as Varied Substrate. When Thy (Q) and dRib-1-P (P) are substrates at [dThd] = [P$_i$] = 0, a double-reciprocal form of eq 3 for 1/v vs. 1/[dRib-1-P] can be represented by

$$1/v = (\text{slope})(1/[P]) + \text{intercept} \qquad (11)$$

where

$$\text{slope} = \frac{\dfrac{1}{[Q]^2} + \dfrac{1}{[Q]}\left(\dfrac{1}{K_{iq}} + \dfrac{1}{K'_q}\right) + \dfrac{1}{K_{iq}K'_{qq}}}{\dfrac{1}{[Q]}\left(\dfrac{V_2}{K_p K_{iq}}\right) + \dfrac{V_4}{K_p K_{iq}K'_{qpq}}}$$

$$\text{intercept} =$$

$$\frac{\dfrac{1}{[Q]^2}\left(\dfrac{1}{K_{ip}}\right) + \dfrac{1}{[Q]}\left(\dfrac{1}{K_p K_{iq}} + \dfrac{1}{K_{ip}K'_{qp}}\right) + \dfrac{1}{K_p K_{iq}K'_{qpq}}}{\dfrac{1}{[Q]}\left(\dfrac{V_2}{K_p K_{iq}}\right) + \dfrac{V_4}{K_p K_{iq}K'_{qpq}}}$$

Equation 11 predicts that, when dRib-1-P is the varied substrate and Thy the changing fixed substrate, the initial velocity plots should be linear. The results shown in Figure 3 are consistent with this prediction. In contrast, the replots of slope and intercept (vs. 1/[Thy]) were not straight lines. The intercept replot curved slightly upward (Figure 3A), and the slope replot curved downward (Figure 3B), as the value of 1/[Thy] increased. This phenomenon is due to binding of Thy to the effector site (see Figure 13) and is reflected in eq 11 by the [Q]^2 terms in the slope and intercept terms. As a result, the initial velocity plots do not intersect at a common point; however, at sufficiently low concentrations of Thy, they appear to have a common intersection.

(2) Thy as Varied Substrate. A double-reciprocal form of eq 3 for 1/v vs. 1/[Thy] takes on the nonlinear form

$$1/v = \frac{(\text{coeff }1)(1/[Q]^2) + (\text{coeff }2)(1/[Q]) + (\text{coeff }3)}{(\text{coeff }4)(1/[Q]) + (\text{coeff }5)} \qquad (12)$$

where

$$\text{coeff }1 = \frac{1}{[P]} + \frac{1}{K_{ip}}$$

$$\text{coeff }2 = \frac{1}{[P]}\left(\frac{1}{K_{iq}} + \frac{1}{K'_q}\right) + \frac{1}{K_p K_{iq}} + \frac{1}{K_{ip}K'_{qp}}$$

$$\text{coeff }3 = \frac{1}{[P]}\left(\frac{1}{K_{iq}K'_{qq}}\right) + \frac{1}{K_p K_{iq}K'_{qpq}}$$

$$\text{coeff }4 = \frac{V_2}{K_p K_{iq}} \qquad \text{coeff }5 = \frac{V_4}{K_p K_{iq}K'_{qpq}}$$

Equation 12 indicates that, in general, a double-reciprocal plot of 1/v vs. 1/[Thy] will not be a straight line. Indeed, when Thy was the varied substrate and dRib-1-P the changing fixed substrate, substrate inhibition by Thy was observed; i.e., as the Thy concentration increased above 0.2 mM, the velocity decreased (Figure 5). These results are consistent with the assumption that binding of Thy to the "effector" site inhibits the catalytic site and as a result $V_4 < V_2$ [Cha, 1968a].

Equation 12 can also be written in the form

$$1/v = \frac{(\text{coeff }1)(1/[Q]) + (\text{coeff }2) + (\text{coeff }3)[Q]}{(\text{coeff }4) + (\text{coeff }5)[Q]} \qquad (13)$$

and at low concentrations of Thy, a linear approximation of eq 13 can be written as

$$1/v = \left(\frac{\text{coeff }1}{\text{coeff }4}\right)\frac{1}{[Q]} + \frac{\text{coeff }2}{\text{coeff }4} \qquad (14)$$
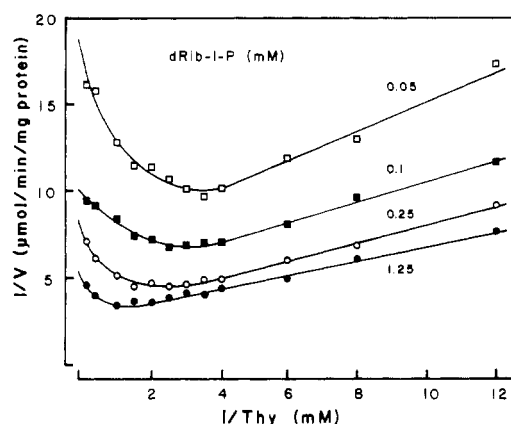
FIGURE 5: Substrate inhibition by Thy. Plots of 1/velocity vs. 1/[Thy] at various fixed concentrations of dRib-1-P. Note that Thy caused substrate inhibition at concentrations higher than 0.25 mM, particularly at low concentrations of dRib-1-P.
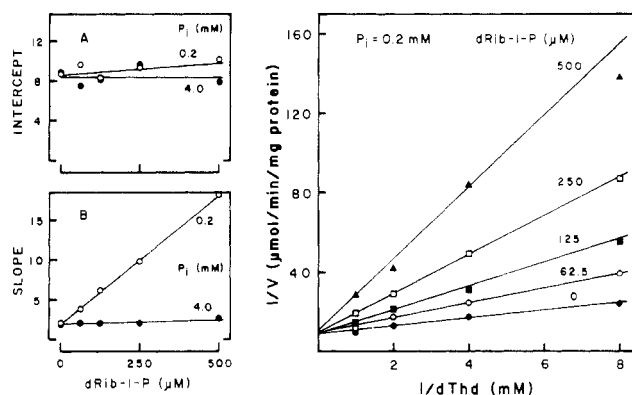

FIGURE 6: Product inhibition by dRib-1-P. Plots of 1/velocity vs. 1/[dThd] at various concentrations of dRib-1-P and a fixed phosphate concentration of 0.2 mM. Insets A and B represent replots of intercept and slope vs. [dRib-1-P], respectively, at phosphate concentrations of 0.2 and 4.0 mM.

Table I: Product Inhibition of Thymidine Phosphorylase

	variable substrate			
	dThd		phosphate	
inhibitory product	0.2 mM phosphate	4 mM phosphate	0.25 mM dThd	5 mM dThd
dRib-1-P	comp[a]	c	comp	c
Thy	comp[b]	comp[b]	noncomp[b]	c

[a] Comp = competitive inhibition; noncomp = noncompetitive. [b] At low concentration of Thy only. [c] No inhibition.

Equation 14 predicts that the initial velocity plots will be nearly linear, when the concentration range of Thy is low enough. When the initial velocity studies were repeated with Thy concentrations at or below 0.25 mM, the initial velocity plots, as well as the intercept and slope replots, were indeed linear (Figure 4). Thus, eq 14 is an approximation of the lines in Figure 4 and the linear portions of the curves in Figure 5.

Product Inhibition Studies. The results of various product inhibition studies are presented in Figures 6–9 and are summarized in Table I. These results are consistent with a rapid equilibrium random bi-bi mechanism, with an enzyme–phosphate–Thy dead-end complex, as originally formulated by Cleland (1963a–c) and shown in Figure 12. However, in order to accommodate the suggested effector site for Thy, the data were analyzed according to the more complex mechanism shown in Figure 13 and the corresponding rate equation (eq 3) derived in the Appendix.
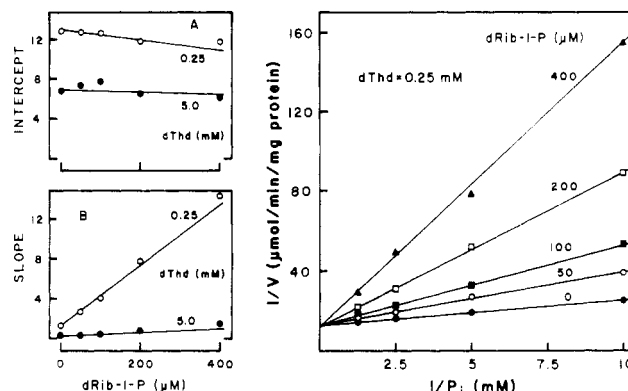

FIGURE 7: Product inhibition by dRib-1-P. Plots of 1/velocity vs. 1/[P_i] at various concentrations of dRib-1-P and a fixed dThd concentration of 0.25 mM. Insets A and B represent replots of intercept and slope vs. [dRib-1-P], respectively, at dThd concentrations of 0.25 and 5.0 mM.
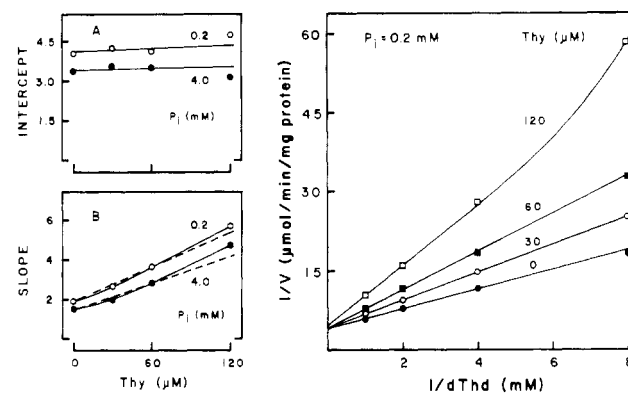
FIGURE 8: Product inhibition by Thy. Plots of 1/velocity vs. 1/[dThd] at various concentrations of Thy and a fixed phosphate concentration of 0.2 mM. Insets A and B represent replots of intercept and slope vs. [Thy], respectively, at phosphate concentrations of 0.2 and 4.0 mM. At a saturating concentration of P_i (4 mM), the x intercept in inset B is an estimate of $K_{i,Thy}$ = 63.5 ± 10.3 μM.
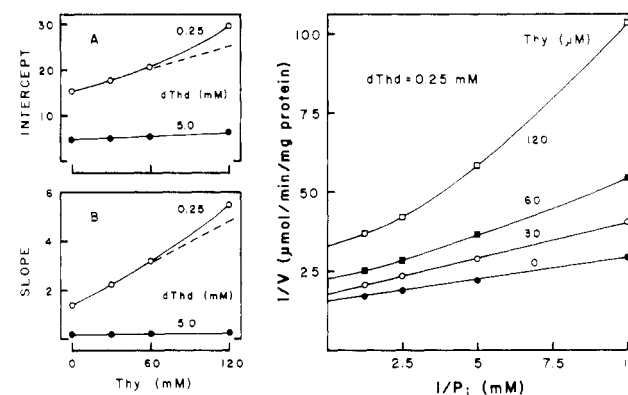
FIGURE 9: Product inhibition by Thy. Plots of 1/velocity vs. 1/[P_i] at various concentrations of Thy and a fixed dThd concentration of 0.25 mM. Insets A and B represent replots of intercept and slope vs. [Thy], respectively, at dThd concentrations of 0.25 and 5.0 mM.

(A) Product Inhibition by dRib-1-P. When dThd (A) and phosphate (B) are substrates in the presence of a finite concentration of dRib-1-P (P) and [Thy] = 0, a double-reciprocal form of eq 3 can be represented by either

$$1/v = \frac{K_a}{V_1}\left[1 + \frac{K_{ib}}{[B]}\left(1 + \frac{[P]}{K_{ip}}\right)\right]\frac{1}{[A]} + \frac{1}{V_1}\left(1 + \frac{K_b}{[B]}\right)$$

(15)

or

$$1/v = \frac{K_b}{V_1}\left[1 + \frac{K_{ia}}{[A]}\left(1 + \frac{[P]}{K_{ip}}\right)\right]\frac{1}{[B]} + \frac{1}{V_1}\left(1 + \frac{K_a}{[A]}\right) \tag{16}$$

dRib-1-P showed competitive inhibition when either dThd (Figure 6) or phosphate (Figure 7) was the varied substrate and the fixed substrate was 0.2 mM phosphate or 0.25 mM dThd, respectively. In both cases, the slopes of the velocity plots increased as the concentration of dRib-1-P increased (Figures 6B and 7B) while the intercepts were essentially the same (Figures 6A and 7A). These results are consistent with eq 15 and 16, which predict that dRib-1-P will affect only the slopes of these plots (i.e., competitive inhibition). At a saturating concentration of the second substrate (either dThd or phosphate), the [P] terms drop out of these equations; therefore, dRib-1-P should no longer be inhibitory. Indeed, when the fixed substrate concentrations were increased to 4 mM phosphate and 5 mM dThd (velocity plots not shown), the inhibition by dRib-1-P was overcome, as indicated by the nearly horizontal slope replots (Figures 6B and 7B).

(B) *Product Inhibition by Thy.* (1) *dThd as the Varied Substrate.* When dThd (A) and phosphate (B) are substrates at a finite concentration of Thy (Q) and [dRib-1-P] = 0, a double-reciprocal form of eq 3 can be expressed as

$$1/v = (\text{slope})(1/[A]) + \text{intercept} \tag{17}$$

where

slope =

$$\left[\frac{1}{[B]}\left(1 + \frac{[Q]}{K_{iq}} + \frac{[Q]}{K'_q} + \frac{[Q]^2}{K_{iq}K'_{qq}}\right) + \frac{1}{K_{ib}} + \frac{[Q]}{K_{ib}K_{ibq}} + \frac{[Q]}{K_{ib}K'_{qb}} + \frac{[Q]^2}{K_{ib}K_{ibq}K'_{qbq}}\right]\Big/\left(\frac{V_1}{K_aK_{ib}} + \frac{V_3[Q]}{K_aK_{ib}K'_{qab}}\right)$$

$$\text{intercept} = \frac{\dfrac{1}{[B]}\left(\dfrac{1}{K_{ia}} + \dfrac{[Q]}{K_{ia}K'_{qa}}\right) + \dfrac{1}{K_aK_{ib}} + \dfrac{[Q]}{K_aK_{ib}K'_{qab}}}{\dfrac{V_1}{K_aK_{ib}} + \dfrac{V_3[Q]}{K_aK_{ib}K'_{qab}}}$$

Equation 17 predicts that plots of $1/v$ vs. $1/[\text{dThd}]$ should be straight lines at all fixed concentrations of Thy. The velocity plots were indeed linear at Thy concentrations of 60 μM or less; however, at concentrations above 60 μM, the plots curved upward (Figure 8). Equation 17 indicates that the intercept replots should be linear, while the replots of slope will not be straight lines due to the $[Q]^2$ terms. This was indeed the case as can be seen in Figure 8. Equation 17 also predicts that Thy should display noncompetitive inhibition with respect to dThd, because [Q] terms are found in both the slope and intercept terms. However, the inhibition pattern observed was essentially competitive as indicated by the nearly horizontal intercept replots (Figure 8A). These results indicate that at the concentrations of Thy employed in these studies binding of Thy to the effector site is negligible (see Figure 13). Equation 17 also predicts that saturation by phosphate will not overcome the inhibition by Thy. Indeed, when the phosphate concentration was increased to 4 mM (velocity plots not shown), the inhibition pattern was not altered, nor was the inhibition by Thy overcome, as indicated by the essentially unchanged slope replot (Figure 8B).

Table II: Estimated Kinetic Constants for Thymidine Phosphorylase

parameter	ligand	value[a]	SE[b]	data source
K_{ia}	dThd	87.2	11.6	Figure 2B
K_a	dThd	288.6	23.5	Figure 2A
K_{ib}	P_i	45.7	6.1	Figure 1B
K_b	P_i	151.2	12.2	Figure 1A
K_{ip}	dRib-1-P	27.1	5.5	Figure 4B
K_p	dRib-1-P	114.0	11.9	Figure 4A
K_{iq}	Thy	41.5	8.8	Figure 3B
K_q	Thy	174.6	16.1	Figure 3A
K_{ibq}	Thy	63.5	10.3	Figure 8B
K_{iqb}	P_i	69.9[c]		
V_1		0.23	0.01	
V_2		0.45	0.02	

[a] μM or μmol min^{-1} (mg of protein)$^{-1}$. [b] Standard error of estimation. [c] Calculated using the identity relationship $K_{ib}K_{ibq} = K_{iq}K_{iqb}$.

(2) *Phosphate as the Varied Substrate.* A double-reciprocal form of eq 3 can also be expressed as

$$1/v = (\text{slope})(1/[B]) + \text{intercept} \tag{18}$$

where

slope =

$$\frac{\dfrac{1}{[A]}\left(1 + \dfrac{[Q]}{K_{iq}} + \dfrac{[Q]}{K'_q} + \dfrac{[Q]^2}{K_{iq}K'_{qq}}\right) + \dfrac{1}{K_{ia}} + \dfrac{[Q]}{K_{ia}K'_{qa}}}{\dfrac{V_1}{K_aK_{ib}} + \dfrac{V_3[Q]}{K_aK_{ib}K'_{qab}}}$$

$$\text{intercept} = \left[\frac{1}{[A]}\left(\frac{1}{K_{ib}} + \frac{[Q]}{K_{ib}K_{ibq}} + \frac{[Q]}{K_{ib}K'_{qb}} + \frac{[Q]^2}{K_{ib}K_{ibq}K'_{qbq}}\right) + \frac{1}{K_aK_{ib}} + \frac{[Q]}{K_aK_{ib}K'_{qab}}\right]\Big/\left(\frac{V_1}{K_aK_{ib}} + \frac{V_3[Q]}{K_aK_{ib}K'_{qab}}\right)$$

Plots of $1/v$ vs. $1/[P_i]$ should be linear at all fixed concentrations of Thy. This was true at low Thy concentrations (30 μM or less). As the Thy concentration increased beyond 30 μM, however, the velocity plots became increasingly nonlinear (Figure 9). The slope and intercept terms in eq 18 predict that at an unsaturating concentration of dThd both replots will be nonlinear because of the $[Q]^2$ terms. At a saturating concentration of dThd, however, these terms will drop out, and the replots should be straight lines. The results shown in Figure 9A,B are consistent with these predictions. Equation 18 also indicates that the inhibition pattern should be noncompetitive and that this inhibition will not be overcome by a saturating concentration of dThd. Thy did display noncompetitive inhibition when phosphate was the varied substrate and the fixed concentration of dThd was 0.25 mM (Figure 9). However, when the dThd concentration was increased to 5 mM, Thy was no longer inhibitory, as indicated by the horizontal intercept and slope replots (Figure 9A,B). These results are consistent with the idea that binding of Thy to the effector site is negligible at the concentrations of Thy employed in these studies.

Estimation of Kinetic Parameters for the Phosphorolytic Reaction. The various kinetic parameters estimated for thymidine phosphorylase are presented in Table II. K_{ia}, K_a, K_{ib}, K_b, and V_1 were calculated from Figures 1 and 2 with eq 9 and 10. Estimates of K_{ip}, K_p, K_{iq}, K_q, and V_2 were obtained from Figures 3 and 4. Because of the complexity of the slope and intercept terms in eq 11 and 12, eq 5 and 6 were used to
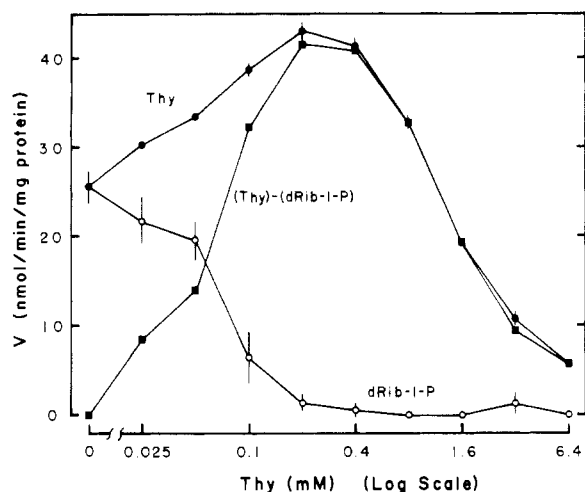
FIGURE 10: Effect of unlabeled Thy on the formation of [U-^{14}C]Thy (●) and [U-^{14}C]dRib-1-P (○) from [U-^{14}C]dThd (0.2 mM) at a phosphate concentration of 0.2 mM. The curve represented by the (■) symbols was obtained by subtracting [U-^{14}C]dRib-1-P formation from [U-^{14}C]Thy formation. The vertical bars represent standard deviation.
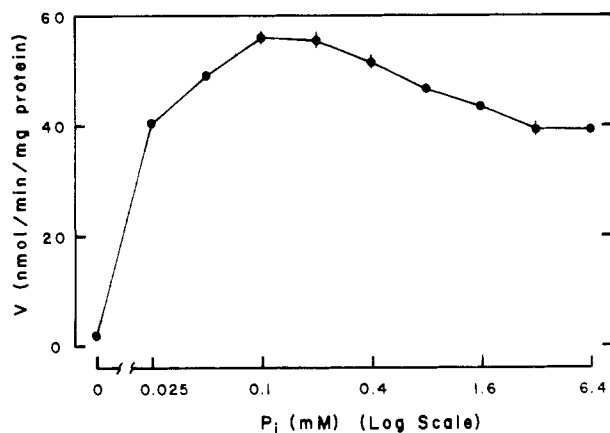

FIGURE 11: Effect of phosphate on deoxyribosyl transferase activity. The unlabeled dThd and [2-^{14}C]Thy concentrations were both 0.2 mM.

calculate these parameters. These estimations are represented by dotted lines in Figures 3 and 4. The kinetic parameter K_{ibq} was calculated from eq 7. At a saturating concentration of phosphate (B), this equation reduces to

$$1/v = \frac{K_a}{V_1}\left(1 + \frac{[Q]}{K_{ibq}}\right)\frac{1}{[A]} + \frac{1}{V_1} \qquad (19)$$

Therefore, the x intercept of Figure 8B, at a phosphate concentration of 4 mM, represents an estimate of K_{ibq}.

Studies on the Deoxyribosyl Transferase Reaction

Effect of Thy. Figure 10 shows the effect of increasing amounts of unlabeled Thy on the production of [U-^{14}C]Thy and [U-^{14}C]dRib-1-P from [U-^{14}C]dThd in the presence of phosphate. In the absence of Thy, the amount of [U-^{14}C]dThy and [U-^{14}C]dRib-1-P formed was equal. When unlabeled Thy was added to the reaction mixture, [U-^{14}C]dRib-1-P formation decreased, while [U-^{14}C]Thy formation increased up to a Thy concentration of 0.2 mM. When the Thy concentration was above 0.2 mM, [U-^{14}C]Thy formation was also inhibited. If dRib-1-P formation is taken as the rate of phosphorolysis of dThd, then by subtracting this rate from the rate of Thy formation (Thy minus dRib-1-P), one can obtain a curve that should represent the rate of Thy formation by the deoxy-

Table III: Effect of Phosphate on the Phosphorylase and Deoxyribosyl Transferase Reactions[a]

enzyme activity[b]	no phosphate[c]	10 mM phosphate	x-fold change[d]
phosphorylase	176.2 ± 9.0	3.4 ± 0.6	−52
deoxyribosyl transferase	6.7 ± 0.6	34.1 ± 1.8	5

[a] Phosphorylase activity was determined by measuring [2-^{14}C]dThd synthesis from [2-^{14}C]Thy (0.2 mM) and unlabeled dRib-1-P (1 mM). Deoxyribosyl transferase activity was determined by measuring [2-^{14}C]dThd synthesis from [2-^{14}C]Thy (0.2 mM) and unlabeled dThd (1 mM). [b] nmol min^{-1} (mg of protein)$^{-1}$. [c] No phosphate was added to the assay; however, there was a residual phosphate contamination of approximately 5 μM. [d] x-fold change in activity in the presence of 10 mM phosphate vs. no added phosphate.

Table IV: Apparent K_m Values for Deoxyribosyl Transferase Activity

substrate[a]	apparent K_m ± SE[b] (μM)
phosphate	19 ± 3
dThd	945 ± 35
Thy	141 ± 5

[a] Fixed substrate concentrations were 10 mM phosphate, 0.2 mM [2-^{14}C]Thy, and 1 mM dThd. [b] Standard error of estimation.

ribosyl-transfer reaction alone as shown in Figure 10.

Effect of Phosphate. The effect of phosphate on deoxyribosyl transferase activity is presented in Figure 11. In the absence of added phosphate, the activity was about 3% that of the maximal activity observed. As the phosphate concentration was increased, the activity increased, reaching a maximum at a phosphate concentration of 0.1–0.2 mM, and then decreased to a plateau between 3.2 and 6.4 mM phosphate.

Table III shows the effect of phosphate on [2-^{14}C]dThd synthesis from [2-^{14}C]Thy and dRib-1-P by the phosphorolytic reaction, as compared to [2-^{14}C]dThd synthesis from [2-^{14}C]Thy and dThd by the deoxyribosyl transferase reaction. As can be seen, 10 mM phosphate strongly inhibited the phosphorolytic reaction by 98%, whereas it stimulated the transferase reaction by 500%.

Apparent K_m Values for the Deoxyribosyl Transferase Reaction. Because Thy and dThd compete for the same binding site on thymidine phosphorylase, it is difficult to measure true kinetic constants for the deoxyribosyl transferase reaction. Therefore, apparent K_m values for phosphate, Thy, and dThd were determined at fixed concentrations of the other two substrates (1 mM dThd, 0.2 mM Thy, and/or 10 mM phosphate). Table IV summarizes the results of these studies.

DISCUSSION

The initial velocity and product inhibition results indicate that the basic reaction mechanism of mouse liver thymidine phosphorylase is a rapid equilibrium random bi-bi mechanism, with an enzyme–phosphate–Thy dead-end complex, as shown in Figure 12. However, this mechanism is not consistent with all of the kinetic data as it cannot explain either the substrate inhibition by Thy or the nonlinear product inhibition. Among the possible mechanisms by which substrate inhibition can occur, the one that is most consistent with the present data is illustrated in Figure 13. This mechanism is based on the following assumptions: (1) thymidine phosphorylase has one catalytic site and one effector site; (2) only Thy binds to the effector site, whereas any of the ligands can bind to the catalytic site; (3) binding of Thy to the effector site inhibits product formation by the catalytic site, i.e., $k_1 > k_3$ and $k_2 > k_4$; (4) the catalytic site has a greater affinity for Thy than
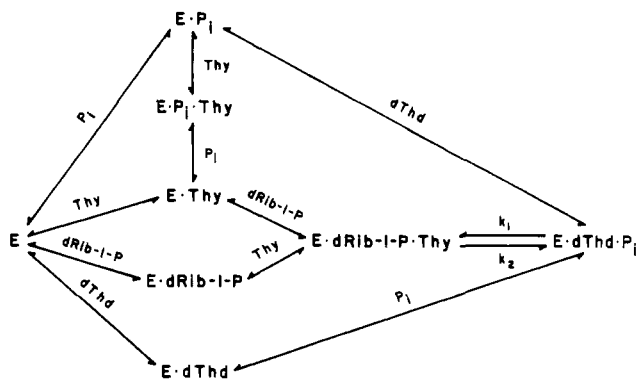
FIGURE 12: Basic reaction mechanism for mouse liver thymidine phosphorylase. This scheme shows a rapid equilibrium random bi-bi mechanism, with an enzyme–phosphate–Thy dead-end complex.
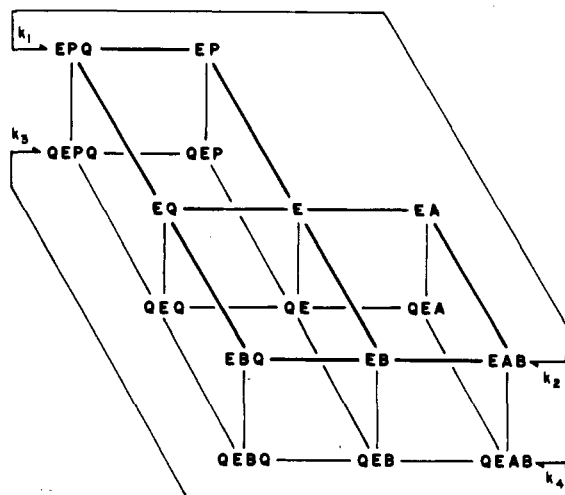

FIGURE 13: Scheme for the reaction catalyzed by mouse liver thymidine phosphorylase. A, B, P, and Q represent dThd, phosphate, dRib-1-P, and Thy, respectively. This model assumes that there is an "effector" site on the enzyme for Thy and that, when Thy is bound to this site, the enzyme is inhibited. The upper level of this figure is the same as that shown in Figure 12, while the lower level consists of enzyme species in which Thy is bound to the "effector" site, which is represented by the letter Q to the left of E.

the effector site. Therefore, as the Thy concentration increases, more and more Thy is bound to the effector site, resulting in (substrate) inhibition of the catalytic site. This mechanism can also account for the nonlinear replots of slope and intercept vs. 1/[Thy], observed in the product inhibition studies (Figures 8 and 9). At low concentrations, Thy inhibits the enzyme by competing with dThd and phosphate for binding to the catalytic site. However, at higher concentrations, Thy also inhibits the enzyme by binding to the effector site.

The only kinetic data that cannot be explained by the scheme shown in Figure 13 are the nonlinear plots of $1/v$ vs. $1/[dThd]$ (Figure 8) or $1/[P_i]$ (Figure 9), in the presence of Thy. These plots indicate that both dThd and phosphate have "cooperative effects" (Monod et al., 1965; Segel, 1975) on thymidine phosphorylase, at least in the presence of Thy. Cooperativity can occur if there is more than one binding site on the enzyme for the substrate and binding of substrate to one site increases the affinity of the other binding sites for the substrate. Therefore, the results shown in Figures 8 and 9 suggest that, in addition to Thy, dThd and phosphate may also have more than one binding site on the enzyme. Thus, thymidine phosphorylase may have multiple interacting allosteric and/or catalytic sites, and the scheme shown in Figure 13 may actually represent only a part of the overall mechanism. However, only those kinetic studies in which Thy was included

as a substrate or product inhibitor displayed subunit interactions in the form of nonlinear velocity plots and/or slope and intercept replots (Figures 3, 5, 8, and 9). Therefore, in order to avoid undue complexity, only those enzyme species that contain Thy bound to the effector site were included in Figure 13 and the corresponding rate equation.

The deoxyribosyl transferase reaction catalyzed by thymidine phosphorylase can be considered as an exchange reaction in which one base moiety (base$_1$) attached to deoxyribose is exchanged for a second base moiety (base$_2$). Although dRib-1-P is an intermediate product in this reaction, there is no net formation of dRib-1-P. On the other hand, the phosphorolytic reaction does produce dRib-1-P in stoichiometric amounts with Thy. One would predict that, in the absence of base$_2$, only the phosphorolytic reaction will occur because the transferase reaction lacks the necessary second substrate. Therefore, formation of Thy and dRib-1-P should be stoichiometric. However, as the concentration of base$_2$ is increased, both reactions can occcur and there will no longer be a stoichiometric relationship between Thy and dRib-1-P, because the transferase reaction "conserves" the deoxyribose moiety. The results shown in Figure 10 are consistent with these predictions. In the absence of added Thy, the amounts of [U-^{14}C]Thy and [U-^{14}C]dRib-1-P formed from [U-^{14}C]dThd were stoichiometric. However, when unlabeled Thy was added, formation of [U-^{14}C]Thy increased, while [U-^{14}C]dRib-1-P formation decreased. dRib-1-P is formed only by the phosphorolytic reaction, whereas Thy can be formed by either phosphorolysis of dThd or the transferase reaction. By subtracting dRib-1-P formation from Thy formation, one can obtain a plot that represents Thy formation by the transferase reaction alone, as shown in Figure 10. When the Thy concentration reaches 0.2 mM, only the transferase reaction is operating; however, when the Thy concentration becomes very high, the transferase reaction is also inhibited due to competition between dThd and Thy for binding to the enzyme.

Figure 11 shows that the deoxyribosyl-transfer reaction is phosphate-dependent. In the absence of added phosphate, the activity was only 3% that of the maximal activity observed. The low level of activity in the absence of added phosphate is probably due to residual phosphate contamination in the enzyme preparation. Since very little phosphate is needed to catalyze deoxyribosyl transfer (apparent K_m value of 19 μM, Table IV), this low requirement for phosphate for the transferase reaction, as compared to the phosphorolytic reaction (K_m = 151 μM, Table II), suggests that a nonstoichiometric amount of phosphate is needed for deoxyribosyl transfer. If deoxyribosyl transfer involves the release of free dRib-1-P, then a stoichiometric amount of phosphate would be required, whereas a nonstoichiometric amount of phosphate would be required if the reaction proceeds via an enzyme-bound dRib-1-P intermediate. It is conceivable that phosphate can "shuttle" back and forth on the enzyme as enzyme-bound phosphate or dRib-1-P. As a result, only a "catalytic" amount of phosphate would be needed for the transferase reaction. Indeed, the instability of thymidine phosphorylase in the presence of low concentrations of phosphate (unpublished result) suggests that phosphate may "never" leave the vicinity of the catalytic site. The results shown in Table III provide further evidence that deoxyribosyl transfer can proceed via an enzyme-bound dRib-1-P intermediate. If dRib-1-P is released from the enzyme (i.e., a free dRib-1-P intermediate), then a saturating concentration of phosphate will inhibit the transfer reaction because it will prevent dRib-1-P from "rebinding" to the enzyme. On the other hand, if dRib-1-P remains bound to the enzyme (i.e., an enzyme-bound inter-

mediate), a saturating concentration of phosphate will not inhibit the transfer reaction. As can be seen in Table III, 10 mM phosphate strongly inhibited dThd synthesis from Thy and "free" dRib-1-P, whereas synthesis of dThd by the deoxyribosyl-transfer reaction was stimulated.

The present study has shown that the deoxyribosyl transferase reaction is phosphate-dependent, requires nonstoichiometric amounts of phosphate, and can proceed via an enzyme-bound dRib-1-P intermediate. All of these results are consistent with the rapid equilibrium random bi-bi mechanism, suggested by the initial velocity and product inhibition studies, and indicate that phosphorolysis and deoxyribosyl transfer are catalyzed by the same site on thymidine phosphorylase. Furthermore, the phosphate dependence of the transfer reaction demonstrates that the reaction proceeds via an indirect transfer mechanism. The random binding of ligands to mouse liver thymidine phosphorylase indicates that the catalytic site of this enzyme may be different from that of other mammalian nucleoside phosphorylases. Rat liver uridine phosphorylase (Kraut & Yamada, 1971), rat lung 5'-methylthioadenosine phosphorylase (Garbers, 1978), and human erythrocytic purine-nucleoside phosphorylase (Kim et al., 1968) have all been shown to have ordered mechanisms, suggesting that the structure of their catalytic sites is such that one substrate must enter the "pocket" before the other. In the case of purine-nucleoside phosphorylase, the crystallographic data that have been obtained to date are in agreement with this idea (Ealick et al., 1985). We hope that several different nucleoside phosphorylases from mammalian sources can be crystallized and analyzed as in the case of human erythrocytic purine-nucleoside phosphorylase to see what causes the difference in substrate specificity and reaction mechanism between these apparently similar enzymes.

APPENDIX

Derivation of Overall Rate Equation. A rate equation was derived for the scheme shown in Figure 13 with rapid equilibrium assumptions (Cha, 1968b; Segel, 1975); i.e., the association and dissociation of ligands to and from the enzyme are in a random order, and these processes occur more rapidly than the interconversion between EAB and EPQ or QEAB and QEPQ. Ligands bound to the catalytic site are represented by letters to the right of E (e.g., EQ), whereas ligands bound to the effector site are represented by letters to the left of E (e.g., QE). We begin with the velocity dependence equation (eq 1), where A, B, P, and Q represent dThd, phosphate,

$$v = k_1[\text{EAB}] + k_3[\text{QEAB}] - k_2[\text{EPQ}] - k_4[\text{QEPQ}] \quad (1)$$

dRib-1-P, and Thy, respectively. The right side of the equation is multiplied by $[E_t]/[E_t]$, where $[E_t]$ represents the total amount of enzyme. The various V_{max} values are defined as

$$V_1 = k_1[E_t] \qquad V_2 = k_2[E_t] \qquad V_3 = k_3[E_t]$$
$$V_4 = k_4[E_t]$$

After substituting these relationships into eq 1 and expressing $[E_t]$ in the denominator as the sum of the concentrations of all enzyme species, the equation becomes

$$v = (V_1[\text{EAB}] + V_3[\text{QEAB}] - V_2[\text{EPQ}] -$$
$$V_4[\text{QEPQ}])/([\text{E}] + [\text{EA}] + [\text{EB}] + [\text{EAB}] + [\text{EBQ}] +$$
$$[\text{EP}] + [\text{EQ}] + [\text{EPQ}] + [\text{QE}] + [\text{QEA}] + [\text{QEB}] +$$
$$[\text{QEAB}] + [\text{QEBQ}] + [\text{QEP}] + [\text{QEQ}] + [\text{QEPQ}]) \quad (2)$$

The concentration of each species is then defined in terms of [E], where K and K' represent the dissociation constants of various E– and QE–ligand complexes, respectively. The K terms in the equations below are defined according to the nomenclature of Cleland (1963a–c). For example, K_{ia} rep-

resents the dissociation constant for the EA complex, and K_a represents the Michaelis constant for A, at a saturating concentration of B. The K' terms, on the other hand, represent the dissociation constants for Q for the effector site when none, one, or two substrates are bound to the catalytic site. For example, K'_q is the dissociation constant for QE → Q + E and K'_{qpq} is the dissociation constant for QEPQ → Q + EPQ:

$$[\text{EA}] = [\text{E}][\text{A}]/K_{ia} \qquad [\text{EB}] = [\text{E}][\text{B}]/K_{ib}$$
$$[\text{EAB}] = [\text{E}][\text{A}][\text{B}]/(K_a K_{ib})$$
$$[\text{EBQ}] = [\text{E}][\text{B}][\text{Q}]/(K_{ib}K_{ibq}) \qquad [\text{EP}] = [\text{E}][\text{P}]/K_{ip}$$
$$[\text{EQ}] = [\text{E}][\text{Q}]/K_{iq} \qquad [\text{EPQ}] = [\text{E}][\text{P}][\text{Q}]/(K_p K_{iq})$$
$$[\text{QE}] = [\text{E}][\text{Q}]/K'_q \qquad [\text{QEA}] = [\text{E}][\text{A}][\text{Q}]/(K_{ia}K'_{qa})$$
$$[\text{QEB}] = [\text{E}][\text{B}][\text{Q}]/(K_{ib}K'_{qb})$$
$$[\text{QEAB}] = [\text{E}][\text{A}][\text{B}][\text{Q}]/(K_a K_{ib}K'_{qab})$$
$$[\text{QEBQ}] = [\text{E}][\text{B}][\text{Q}]^2/(K_{ib}K_{ibq}K'_{qbq})$$
$$[\text{QEP}] = [\text{E}][\text{P}][\text{Q}]/(K_{ip}K'_{qp})$$
$$[\text{QEQ}] = [\text{E}][\text{Q}]^2/(K_{iq}K'_{qq})$$
$$[\text{QEPQ}] = [\text{E}][\text{P}][\text{Q}]^2/(K_p K_{iq}K'_{qpq})$$

When these relationships are substituted into eq 2 and [E] is factored out, the overall rate equation (eq 3) is obtained.

$$v = \left(\frac{V_1[\text{A}][\text{B}]}{K_a K_{ib}} + \frac{V_3[\text{A}][\text{B}][\text{Q}]}{K_a K_{ib}K'_{qab}} - \frac{V_2[\text{P}][\text{Q}]}{K_p K_{iq}} - \right.$$
$$\left. \frac{V_4[\text{P}][\text{Q}]^2}{K_p K_{iq}K'_{qpq}} \right) \Big/ \left(1 + \frac{[\text{A}]}{K_{ia}} + \frac{[\text{B}]}{K_{ib}} + \frac{[\text{A}][\text{B}]}{K_a K_{ib}} + \right.$$
$$\frac{[\text{B}][\text{Q}]}{K_{ib}K_{ibq}} + \frac{[\text{P}]}{K_{ip}} + \frac{[\text{Q}]}{K_{iq}} + \frac{[\text{P}][\text{Q}]}{K_p K_{iq}} + \frac{[\text{Q}]}{K'_q} + \frac{[\text{A}][\text{Q}]}{K_{ia}K'_{qa}} +$$
$$\frac{[\text{B}][\text{Q}]}{K_{ib}K'_{qb}} + \frac{[\text{A}][\text{B}][\text{Q}]}{K_a K_{ib}K'_{qab}} + \frac{[\text{B}][\text{Q}]^2}{K_{ib}K_{ibq}K'_{qbq}} + \frac{[\text{P}][\text{Q}]}{K_{ip}K'_{qp}} +$$
$$\left. \frac{[\text{Q}]^2}{K_{iq}K'_{qq}} + \frac{[\text{P}][\text{Q}]^2}{K_p K_{iq}K'_{qpq}} \right) \quad (3)$$

Although eq 3 is very useful in explaining the effects of Thy bound to the effector site, it cannot be used to estimate kinetic parameters, due to the complexity of the various slope and intercept replots. A simplified version of eq 3 can be derived if certain assumptions are made. If Thy binds to the effector site much less tightly than to the catalytic site, then at low concentrations of Thy the terms responsible for such bindings (i.e. the K' terms) can be neglected and the rate equation becomes

$$v = \left(\frac{V_1[\text{A}][\text{B}]}{K_a K_{ib}} - \frac{V_2[\text{P}][\text{Q}]}{K_p K_{iq}} \right) \Big/ \left(1 + \frac{[\text{A}]}{K_{ia}} + \frac{[\text{B}]}{K_{ib}} + \right.$$
$$\left. \frac{[\text{A}][\text{B}]}{K_a K_{ib}} + \frac{[\text{B}][\text{Q}]}{K_{ib}K_{ibq}} + \frac{[\text{P}]}{K_{ip}} + \frac{[\text{Q}]}{K_{iq}} + \frac{[\text{P}][\text{Q}]}{K_p K_{iq}} \right) \quad (4)$$

Equation 4 represents the rate equation for the basic mechanism depicted in Figure 12. When dThd and phosphate are substrates at [dRib-1-P] = [Thy] = 0, the double-reciprocal forms of eq 4 are the same as eq 9 and 10 (see Results). When Thy and dRib-1-P are substrates at [dThd] = [P_i] = 0, the double-reciprocal forms of eq 4 are

$$1/v = \frac{K_p}{V_2}\left(1 + \frac{K_{iq}}{[\text{Q}]} \right)\frac{1}{[\text{P}]} + \frac{1}{V_2}\left(1 + \frac{K_q}{[\text{Q}]} \right) \quad (5)$$

and

$$1/v = \frac{K_q}{V_2}\left(1 + \frac{K_{ip}}{[P]}\right)\frac{1}{[Q]} + \frac{1}{V_2}\left(1 + \frac{K_p}{[P]}\right) \qquad (6)$$

When dThd and phosphate are substrates at a finite concentration of dRib-1-P and [Thy] = 0, the double-reciprocal forms of eq 4 are the same as eq 15 and 16 (see Results). When dThd and phosphate are substrates at a finite concentration of Thy and [dRib-1-P] = 0, the double-reciprocal forms of eq 4 are

$$1/v =$$
$$\frac{K_a}{V_1}\left[1 + \frac{K_{ib}}{[B]}\left(1 + \frac{[Q]}{K_{iq}}\right) + \frac{[Q]}{K_{ibq}}\right]\frac{1}{[A]} + \frac{1}{V_1}\left(1 + \frac{K_b}{[B]}\right)$$
$$(7)$$

and

$$1/v = \frac{K_b}{V_1}\left[1 + \frac{K_{ia}}{[A]}\left(1 + \frac{[Q]}{K_{iq}}\right)\right]\frac{1}{[B]} +$$
$$\frac{1}{V_1}\left[1 + \frac{K_a}{[A]}\left(1 + \frac{[Q]}{K_{ibq}}\right)\right] \qquad (8)$$

In Figures 3, 8, and 9, the dotted lines represent estimates of the slope and intercept replots calculated from eq 5–8.

Registry No. dThd, 50-89-5; P$_i$, 14265-44-2; dRib-1-P, 17039-17-7; Thy, 65-71-4; thymidine phosphorylase, 9030-23-3.

REFERENCES

Bio-Rad Laboratories (1979) *Bio-Rad Laboratories Bulletin* 1069, Bio-Rad Laboratories, Richmond, CA.

Blank, J. G., & Hoffee, P. A. (1975) *Arch. Biochem. Biophys.* *168*, 259.

Bradford, M. M. (1976) *Anal. Biochem. 72*, 248.

Cha, S. (1968a) *Mol. Pharmacol. 4*, 621.

Cha, S. (1968b) *J. Biol. Chem. 243*, 820.

Cleland, W. W. (1963a) *Biochim. Biophys. Acta 67*, 104.

Cleland, W. W. (1963b) *Biochim. Biophys. Acta 67*, 173.

Cleland, W. W. (1963c) *Biochim. Biophys. Acta 67*, 188.

Cleland, W. W. (1967) *Adv. Enzymol. Relat. Areas Mol. Biol. 29*, 1.

Desgranges, C., Razaka, G., Rabaud, M., & Bricaud, H. (1981) *Biochim. Biophys. Acta 654*, 211.

Ealick, S. E., Greenhough, T. J., Babu, Y. S., Carter, D. C., Cook, W. J., Bugg, C. E., Rule, S. A., Habash, J., Helliwell, J. R., Stoeckler, J. D., Chen, S. F., & Parks, R. E. (1985) *Ann. N.Y. Acad. Sci.* (in press).

Ferone, R., Bushby, S. R. M., Burchall, J. J., Moore, W. D., & Smith, D. (1975) *Antimicrob. Agents Chemother. 7*, 91.

Friedkin, M., & Roberts, D. (1954) *J. Biol. Chem. 207*, 245.

Gallo, R. C., & Breitman, T. R. (1968) *J. Biol. Chem. 243*, 4936.

Gallo, R. C., & Perry, S. (1969) *J. Clin. Invest. 48*, 105.

Gallo, R. C., Perry, S., & Breitman, T. R. (1967) *J. Biol. Chem. 242*, 5059.

Garbers, D. L. (1978) *Biochim. Biophys. Acta 523*, 82.

Giles, K. W., & Myers, A. (1965) *Nature (London) 206*, 93.

Iltzsch, M. H. (1985) Ph.D. Thesis, Brown University.

Iltzsch, M. H., el Kouni, M. H., & Cha, S. (1985) *Proc. Am. Assoc. Cancer Res. 25.*

Kim, B. K., Cha, S., & Parks, R. E. (1968) *J. Biol. Chem. 243*, 1763.

Kono, A., Hara, Y., Sugata, S., Karube, Y., Matsushima, Y., & Ishitsuka, H. (1983) *Chem. Pharm. Bull. 31*, 175.

Kraut, A., & Yamada, E. W. (1971) *J. Biol. Chem. 246*, 2021.

Krenitsky, T. A. (1968) *J. Biol. Chem. 243*, 2871.

Krenitsky, T. A., Barclay, M., & Jacquez, J. A. (1964) *J. Biol. Chem. 239*, 805.

Kubilus, J., Lee, L. D., & Baden, H. P. (1978) *Biochim. Biophys. Acta 527*, 221.

Lyon, G. M. (1968) *Biochim. Biophys. Acta 159*, 38.

Monod, J., Wyman, J., & Changeux, J.-P. (1965) *J. Mol. Biol. 12*, 88.

Nakayama, C., Wataya, Y., Meyer, R. B., & Santi, D. V. (1980) *J. Med. Chem. 23*, 962.

Niedzwicki, J. G., el Kouni, M. H., Chu, S. H., & Cha, S. (1983) *Biochem. Pharmacol. 32*, 399.

Schwartz, M. (1971) *Eur. J. Biochem. 21*, 191.

Segel, I. H. (1975) *Enzyme Kinetics*, pp 22–24, 353–377, Wiley-Interscience, New York.

Wilkinson, G. N. (1961) *Biochem. J. 80*, 321.

Zimmerman, M. (1962) *Biochem. Biophys. Res. Commun. 8*, 169.

Zimmerman, M. (1964) *J. Biol. Chem. 239*, 2622.

Zimmerman, M., & Seidenberg, J. (1964) *J. Biol. Chem. 239*, 2618.